Available online at www.sciencedirect.com
ScienceDirect
International Journal of Heat and Mass Transfer 50 (2007) 2117–2123
International Journal of HEAT and MASS TRANSFER
www.elsevier.com/locate/ijhmt

Transient temperature and thermal stress profiles in semi-transparent particles under high-flux irradiation

Leonid Dombrovsky [a,*], Wojciech Lipiński [b]

[a] Institute for High Temperatures of the Russian Academy of Sciences, Krasnokazarmennaya 17A, NCHMT, Moscow 111116, Russia
[b] Department of Mechanical and Process Engineering, ETH Zurich, 8092 Zurich, Switzerland

Received 19 September 2006; received in revised form 30 October 2006
Available online 28 December 2006

Abstract

Transient temperature and thermal stress profiles in semi-transparent spherical particles heated by concentrated solar radiation are studied by means of a theoretical model. The analysis of radiative–conductive interaction is based on the spectral radiation transfer model in a refracting and absorbing particle. The stress–strain state of the particle is described by the thermoelastic approach. An analytical self-similar solution for the particle temperature profiles and thermal stresses during the quasi-steady period of the particle heating is derived. It is shown that the circumferential tensile stress near the particle surface is a non-monotonic function of the particle radius. The range of physical parameters corresponding to the maximal tensile stress near the particle surface is determined. The model is applied to ZnO and $CaCO_3$ particles, which are used as reactants in industrially-relevant high-temperature processes. It is shown that tensile stresses in the selected types of particles exposed to concentrated solar radiation cannot lead to their mechanical destruction. At the same time, the considerable temperature difference and thermal stresses in non-isothermal particles can be an interesting issue in a detailed analysis of the thermal decomposition of semi-transparent particles.

Keywords: Radiation; Conduction; Transient; Thermal stresses; Particle; Semi-transparent; Solar energy

1. Introduction

Heterogeneous participating media containing large particles that are semi-transparent in the visible and infrared spectral ranges and exposed to intense thermal radiation are encountered in a wide range of high-temperature applications. Examples include plasma spraying [1,2], heating and combustion of liquid fuel droplets [3], water droplet curtains for shielding from fire radiation [4], and selected solar thermochemical processes [5,6]. In a single semi-transparent particle radiation is non-uniformly absorbed and the maximum of absorption is displaced from the particle surface. More intensive heating and thermal expansion of the internal region of a solid particle generates tensile stresses at the particle periphery, which may exceed the failing strength of the particle material and cause mechanical destruction of the particle. In chemically reacting flows the rate of heterogeneous reaction will be influenced by the changing particle size distribution.

In the present paper, the temperature and maximum local tensile stress within semi-transparent particles are analysed with respect to the particle material properties and size [7]. The mathematical formulation includes the modified differential approximation of the radiative transfer equation, the thermoelastic stress–strain relations, and an unsteady energy equation linking the conductive and radiative heat transfer modes. Aside from the general analytical and numerical analysis of the problem, numerical results are obtained for small, micron-sized ZnO and large $CaCO_3$ particles, both used as reactants in high-temperature solar thermochemical reactions [5,6].

* Corresponding author. Tel.: +7 495 362 5590/250 3264; fax: +7 495 362 5590.
E-mail address: dombr@online.ru (L. Dombrovsky).

0017-9310/$ - see front matter © 2006 Published by Elsevier Ltd.
doi:10.1016/j.ijheatmasstransfer.2006.11.008

Nomenclature

a	particle radius, m
D	dimensionless radiation diffusion coefficient
E	Young's modulus, Pa
f	function defined by Eq. (23)
g_0	unknown function in Eq. (4)
I_λ	spectral radiation intensity, W m^{-3} sr^{-1}
k	index of absorption
k_c	thermal conductivity, W m^{-1} K^{-1}
n	index of refraction
p	dimensionless power parameter
q	radiative flux, W m^{-2}
Q	total absorbed power per unit volume, W m^{-3}
Q_a	efficiency factor of absorption
r	radial coordinate, m
s	dependent variable introduced by Eq. (20)
t	time, s
T	temperature, K
u	radial displacement, m
w	normalized local absorption
W	normalized total absorption

Greek symbols

α	linear coefficient of thermal expansion, K^{-1}
Θ	Heaviside unit step function
κ	absorption coefficient, m^{-1}
λ	wavelength, m
μ	directional cosine of the polar angle
ν	Poison's ratio
σ_r, σ_θ, σ_ϕ	stress components, Pa

Subscripts

a	absorption
b	blackbody
bulk	bulk
e	external
m	maximum
s	radiation source
λ	spectral
0	initial

Overbar

$\bar{}$	dimensionless quantity

2. Radiation absorption in a semi-transparent spherical particle

The general solution for radiation absorption in a homogeneous spherical particle at arbitrary asymmetric illumination can be obtained on the basis of the Mie theory [8,9]. In the case of large particles, one can ignore the wave effects, which are important for particles of radius a comparable with the radiation wavelength λ, and use the geometrical optics approximation for determining the distribution of absorbed radiation power in the particle. The exact solution for an arbitrary particle illumination is very complicated even for large particles. Thus, approximate solution methods are usually considered [10]. The present analysis is reduced to the case of spherically symmetric illumination, having in mind probable rotation of the moving particles. To simplify the problem, it is assumed that both the index of refraction n_λ and the index of absorption k_λ of the particle substance do not depend on temperature, and hence, on the location in the particle.

The variation of radiative intensity within a large homogeneous particle is described by the radiative transfer theory. Also, due to moderate temperature ranges required by the thermo-mechanical analysis presented later, the thermal radiation of heated particles is neglected. For a spherical particle, the equation of radiative transfer and the corresponding boundary conditions read [11],

$$\mu\frac{\partial I_\lambda}{\partial r}+\frac{1-\mu^2}{r}\frac{\partial I_\lambda}{\partial \mu}+\kappa_\lambda I_\lambda=0, \tag{1}$$

$$I_\lambda(0,\mu)=I_\lambda(0,-\mu), \tag{2}$$

$$I_\lambda(a,\mu)=\rho_\lambda(\mu)I_\lambda(a,-\mu)+[1-\rho_\lambda(\mu)]I_{\lambda,e},\ \mu>0, \tag{3}$$

where μ is the directional cosine of the polar angle measured from the normal directed into the particle and $\kappa_\lambda=4\pi k_\lambda/\lambda$ is the absorption coefficient of the particle material. For semi-transparent materials $n_\lambda \gg k_\lambda$, and the effect of particle absorption on the refraction and reflection at the interface between the particle and the ambient medium becomes negligible. The spectral directional-hemispherical reflectivity of the interface, $\rho_\lambda(\mu,n_\lambda)$, is obtained from Fresnel's equation for unpolarised incident radiation [12].

In the case of the spherically symmetric illumination of a particle, the radial distribution of absorbed power coincides with the profile of radiation power generated by an isothermal particle. An analysis of radiative transfer inside a homogeneous semi-transparent particle [13,14] showed different behaviour of the angular dependences of the radiative intensity at different locations. In the central zone $r<r_*=a/n$ this angular dependence can be well described by the usual DP_0-approximation of the double spherical harmonics [15], whereas in the periphery of the particle $r_*<r<a$ the reflection of radiation from the particle

surface leads to more complex angular distribution. To solve the problem in the whole volume of the particle, a modified approximation called MDP_0 was developed [1]. As shown in [1], MDP_0 gives sufficiently accurate results for the radiation field inside a semi-transparent particle, whereas the computational time is reduced by two orders of magnitude compared to that required by the direct numerical solution of the equation of radiative transfer.

For an externally and symmetrically irradiated particle, the application of the MDP_0 approximation leads to the boundary-value problem for function $g_0(\bar{r})$ in the following form [10]:

$$\frac{1}{\bar{r}^2}(\bar{r}^2 D_\lambda g_0')' - (1-\mu_*)\tau_\lambda^2 g_0 = 0,$$
$$g_0'(0) = 0,$$
$$D_\lambda g_0'(1) = \tau_\lambda \frac{4n_\lambda^2 - g_0(1)}{n_\lambda(n_\lambda^2+1)}. \quad (4)$$

In the above equation, $\bar{r} = r/a$ is the dimensionless radius, $D_\lambda = \frac{1+\mu_*}{4}(1-\mu_*^2)$ is the dimensionless radiation diffusion coefficient, $\mu_* = \sqrt{1-(\bar{r}_*/\bar{r})^2}\Theta(\bar{r}-\bar{r}_*)$ is a limiting directional cosine of the cone angle, $\Theta(\bar{r}-\bar{r}_*)$ is Heaviside's unit step function, and $\tau_\lambda = \kappa_\lambda a$ is the spectral optical thickness of the particle. The function $g_0(r)$ is proportional to the radiation energy density:

$$g_0(\bar{r}) \sim \int_{-1}^{1} I_\lambda(\bar{r},\mu)\mathrm{d}\mu. \quad (5)$$

The radial distribution of radiative power absorbed in a spherical particle is characterized by the normalized profile of absorption $w_\lambda(\bar{r})$. For a rotating particle illuminated from one side, it coincides with the profile of radiative power generated inside an isothermal particle, and is given by [10]

$$w_\lambda(\bar{r}) = \frac{(1-\mu_*)g_0(\bar{r})}{3\int_0^1 (1-\mu_*)g_0(\bar{r})\bar{r}^2\mathrm{d}\bar{r}}. \quad (6)$$

Obviously, $w_\lambda(\bar{r})$ depends only on two dimensionless spectral parameters: the index of refraction n_λ and the particle optical thickness τ_λ [1,10]. The power absorbed in a rotating particle illuminated from one side by the concentrated solar radiation with the spectrum of the blackbody at temperature T_s can be calculated as follows [10]:

$$Q(\bar{r}) = \frac{1.5\pi}{a}\frac{q_e}{\sigma T_s^4}\int_0^\infty Q_a w_\lambda(\bar{r}) I_{b\lambda}(T_s)\mathrm{d}\lambda. \quad (7)$$

The absorption efficiency factor Q_a of a large semi-transparent particle is well approximated by [3]:

$$Q_a = \frac{4n_\lambda}{(n_\lambda+1)^2}[1-\exp(-2\tau_\lambda)]. \quad (8)$$

3. Transient radiative–conductive heat transfer

For the purpose of better elucidating the thermal response of the particle to the incoming radiation, the convective heat transfer between the particle and the ambient medium is omitted from the analysis. The transient temperature profile in the particle $T(t,r)$ is determined by solving for the coupled radiative–conductive heat transfer inside the particle. The governing energy equation and the corresponding boundary and initial conditions are given by

$$\rho c\frac{\partial T}{\partial t} = \frac{1}{r^2}\frac{\partial}{\partial r}\left(r^2 k_c \frac{\partial T}{\partial r}\right) + Q(r), \quad (9)$$

$$T(r,t=0) = T_0; \quad \left.\frac{\partial T}{\partial r}\right|_{r=0} = 0; \quad \left.\frac{\partial T}{\partial r}\right|_{r=a} = 0. \quad (10)$$

This is a particular case of the general radiative–conductive problem for a moving particle considered previously in [2]. Inserting Eq. (7) into (9) and ignoring the temperature dependence of the thermal conductivity k_c and volumetric heat capacity ρc, non-dimensional forms of Eqs. (9) and (10) are derived,

$$\frac{\partial \overline{T}}{\partial \bar{t}} = \frac{1}{\bar{r}^2}\frac{\partial}{\partial \bar{r}}\left(\bar{r}^2\frac{\partial \overline{T}}{\partial \bar{r}}\right) + 1.5\frac{\pi p}{\sigma T_s^4}\int_0^\infty Q_a w_\lambda(\bar{r}) I_{\lambda b}(T_s)\mathrm{d}\lambda, \quad (11)$$

$$\overline{T}(\bar{r},t=0) = 0; \quad \left.\frac{\partial \overline{T}}{\partial \bar{r}}\right|_{\bar{r}=0} = \left.\frac{\partial \overline{T}}{\partial \bar{r}}\right|_{\bar{r}=1} = 0, \quad (12)$$

where $\bar{t} = k_c t/(\rho c a^2)$, $\overline{T} = T/T_0 - 1$, $p = q_e a/(k_c T_0)$. As can be observed in Eq. (11), the dimensionless temperature $\overline{T}$ is directly proportional to the power parameter p.

4. Thermoelastic stress–strain state

Due to the spherical symmetry, the only non-zero displacement component is the radial displacement $u(r)$ and the only non-zero stress components are the radial stress σ_r and the circumferential stresses $\sigma_\theta = \sigma_\phi$. The thermo-mechanical analysis is limited to the initial period of heating, when the particle still remains at moderate temperature. This condition enables one to simplify the problem by considering only the elastic behaviour of the particle material. Particle heating beyond the upper limit of the elastic range does not lead to considerable thermal stresses. Taking the thermo-mechanical properties of the particle substance being independent of temperature, one can derive the following boundary-value problem for the dimensionless displacement $\bar{u}(\bar{t},\bar{r}) = u(\bar{t},\bar{r})/(\alpha T_0)$ [16]:

$$\frac{1}{\bar{r}^2}\frac{\partial}{\partial \bar{r}}\left(\bar{r}^2\frac{\partial \bar{u}}{\partial \bar{r}}\right) - \frac{2\bar{u}}{\bar{r}^2} = \frac{1+\nu}{1-\nu}\frac{\partial \overline{T}}{\partial \bar{r}}, \quad (13)$$

$$\bar{u}(\bar{r}=0) = 0, \quad \left.\frac{\partial \bar{u}}{\partial \bar{r}}\right|_{\bar{r}=1} = \frac{1+\nu}{1-\nu}\overline{T}(1,\bar{t}) - \frac{2\nu}{1-\nu}\bar{u}(1,\bar{t}), \quad (14)$$

where α is the linear coefficient of thermal expansion and ν is the Poisson's ratio. The dimensionless time $\bar{t}$ is used only as a parameter. After the calculation of the radial displacement, the dimensionless stress components can be determined using the following equations:

$$\bar{\sigma}_r(\bar{r},\bar{t}) = \frac{\sigma_r}{\alpha T_0 E} = \frac{1}{1-2\nu}\left[\frac{1-\nu}{1+\nu}\frac{\partial \bar{u}}{\partial \bar{r}} + \frac{2\nu}{1+\nu}\frac{\bar{u}}{\bar{r}} - \overline{T}\right], \quad (15)$$

$$\bar{\sigma}_\theta(\bar{r},\bar{t}) = \frac{\sigma_\theta}{\alpha T_0 E} = \frac{1}{1-2\nu}\left[\frac{\nu}{1+\nu}\frac{\partial \bar{u}}{\partial \bar{r}} + \frac{1}{1+\nu}\frac{\bar{u}}{\bar{r}} - \overline{T}\right], \quad (16)$$

where E is the Young's modulus. Obviously, the stress components are proportional to the dimensionless temperature $\overline{T}$, and thus, to the power parameter p. Of particular interest is the circumferential stress component at the particle surface, $\bar{\sigma}_1(\bar{t}) = \bar{\sigma}_\theta(1,\bar{t})$, which is expected to be responsible for a possible mechanical destruction of the particle.

5. Generalised analysis of the problem

For a physical analysis of thermal stresses in an arbitrary semi-transparent particle heated by external radiation, it is convenient to use a spectrally-averaged index of refraction n and particle optical thickness τ. Hence, the spectral dependence in Eqs. (4) and (6) can be omitted, and only one function $w(\bar{r})$ needs to be evaluated. The energy Eq. (11) simplifies to

$$\frac{\partial \overline{T}}{\partial \bar{t}} = \frac{1}{\bar{r}^2}\frac{\partial}{\partial \bar{r}}\left(\bar{r}^2\frac{\partial \overline{T}}{\partial \bar{r}}\right) + 1.5pQ_a w(\bar{r}), \quad \overline{T}(\bar{r},\bar{t}=0) = 0,$$

$$\left.\frac{\partial \overline{T}}{\partial \bar{r}}\right|_{\bar{r}=0} = 0, \quad \left.\frac{\partial \overline{T}}{\partial \bar{r}}\right|_{\bar{r}=1} = 0. \quad (17)$$

The transient problem (17) is solved simultaneously with Eqs. (4), (6), and (8) by applying the implicit finite-difference scheme on a uniform grid consisting of 100 radial intervals for either 100 or 200 time steps. The functions $w(\bar{r})$ for $n = 2$ and various values of the optical thickness are shown in Fig. 1. In the case of optically thin particle, the radiation is absorbed mainly in the central region of radius $\bar{r} < 1/n$. Similar results were reported in [10] for other values of the refractive index. The time variation of the particle temperature for the case of $n = 2$ is illustrated

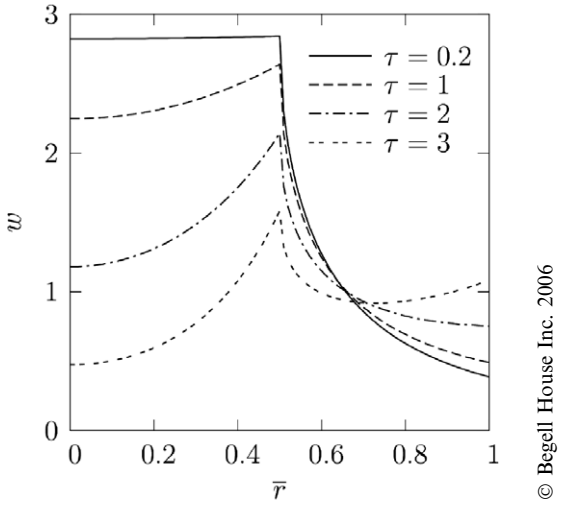

Fig. 1. Radial profiles of absorbed radiative power (Figs. 1–8 are reprinted from [7], Copyright (2006), with permission from Begell House, Inc.).

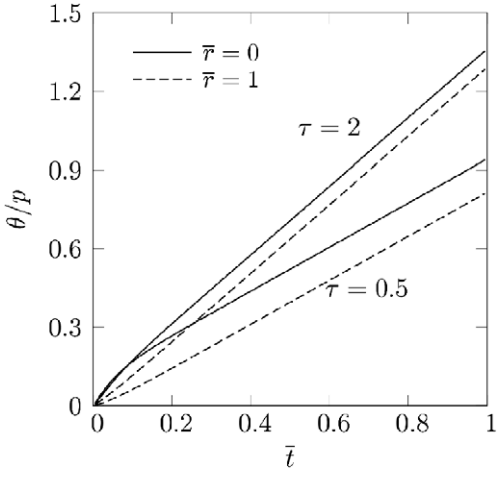

Fig. 2. Time variation of the temperature at the centre and surface of a particle.

in Fig. 2. One can see that temperature difference $\Delta\overline{T}(\bar{t}) = \overline{T}(\bar{r}=0,\bar{t}) - \overline{T}(\bar{r}=1,\bar{t})$ remains approximately constant during the main part of the process. It is a self-similar regime of the particle heating when the bulk temperature increases linearly with time and the temperature profiles at different time moments are similar to each other. The typical temperature profiles are shown in Fig. 3. In the self-similar regime, there is no need for the numerical solution of the energy equation. Instead, one can estimate the bulk temperature of the particle and the temperature difference using the following equations:

$$\overline{T}_{\text{bulk}}(\bar{t}) = 3\int_0^1 \overline{T}(\bar{r},\bar{t})\bar{r}^2 \mathrm{d}r = 1.5pQ_a\bar{t}, \quad (18)$$

$$\Delta\overline{T} = \frac{pQ_a}{4}\left[2\int_0^1 \frac{W(\bar{r})}{\bar{r}^2}\mathrm{d}r - 1\right], \quad (19)$$

where $W(\bar{r}) = 3\int_0^{\bar{r}} w(\bar{r})\bar{r}^2 \mathrm{d}\bar{r}$.

The effect of the particle optical properties on the quasi-steady temperature difference between the centre and the surface of the particle is illustrated in Fig. 4. The overheat-

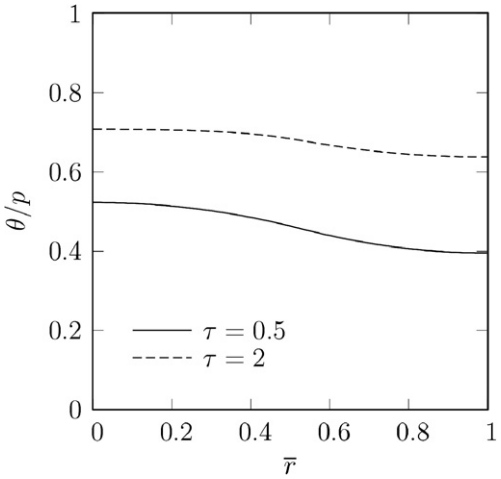

Fig. 3. Radial temperature profiles at $\bar{t} = 0.5$.

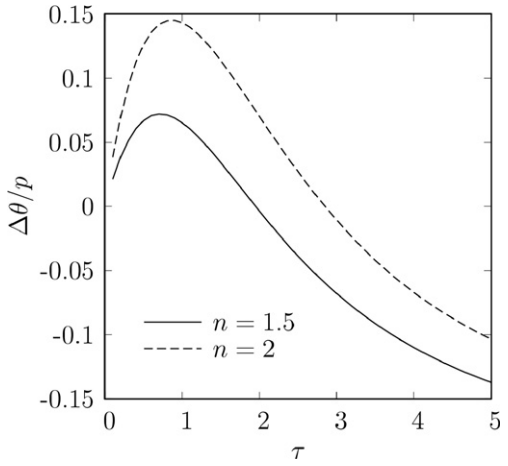

Fig. 4. Quasi-steady temperature difference as a function of the particle optical thickness.

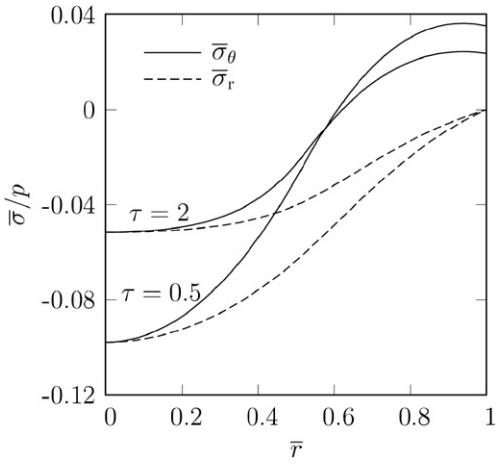

Fig. 5. Radial profiles of the radial and circumferential stress components.

ing of the particle central region is observed at relatively small optical thickness and reaches the maximum at $\tau \approx 0.8$.

In the analysis of thermal stresses, we consider the most important self-similar regime. It is convenient to introduce a new dependent variable $s(\bar{r})$ by using the expression

$$\bar{u}(\bar{r}) = \overline{T}_{\text{bulk}}\bar{r} + \Delta\overline{T}s(\bar{r}), \tag{20}$$

and transform Eqs. (13)–(16) to the following ones:

$$\frac{1}{\bar{r}^2}(\bar{r}^2 s')' - \frac{2s}{\bar{r}^2} = \frac{1+v}{1-v}f'(\bar{r}), \quad s(0) = 0,$$
$$s'(1) = \frac{1+v}{1-v}f(1) - \frac{2v}{1-v}s(1), \tag{21}$$
$$\bar{\sigma}_r(\bar{r}) = \frac{\Delta\theta}{1-2v}\left[\frac{(1-v)s' + 2vs/\bar{r}}{1+v} - f\right],$$
$$\bar{\sigma}_\theta(\bar{r}) = \frac{\Delta\theta}{1-2v}\left[\frac{vs' + s/\bar{r}}{1+v} - f\right], \tag{22}$$

where

$$f(\bar{r}) = \left[\bar{r}^2 - 2\int_0^{\bar{r}} \frac{W(\bar{r})}{\bar{r}^2}\mathrm{d}\bar{r}\right] \Big/ \left[2\int_0^1 \frac{W(\bar{r})}{\bar{r}^2}\mathrm{d}\bar{r} - 1\right], \tag{23}$$

and $\Delta\overline{T}$ can be determined by using Eq. (19). One can see that the thermal stress components are independent of time and directly proportional to $\Delta\overline{T}$.

The calculated radial profiles of the stress components for $n = 2$ and $v = 0.3$ are presented in Fig. 5. The positive values of $\bar{\sigma}_\theta$ at the particle periphery ($\bar{r} > 0.6$) are the tensile stresses which may lead to the particle destruction. The tensile stress at the particle surface is plotted in Fig. 6 as a function of the particle optical thickness for the selected values of the refractive index. The curves follow those of the temperature difference shown in Fig. 4 for the corresponding values of n. For the fixed power parameter p, the maximal tensile stress is observed for particles of optical thickness $\tau \approx 0.8$.

The tensile stress at the particle surface can be estimated by using the following equation:

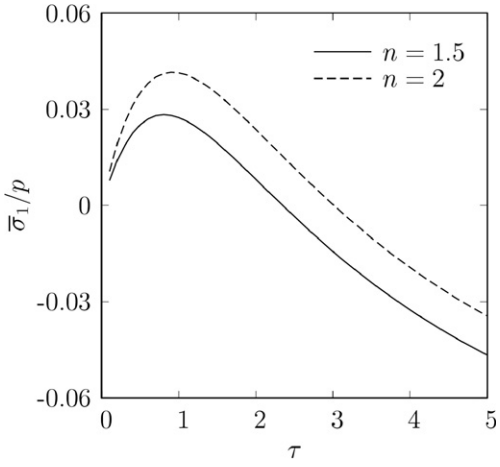

Fig. 6. The circumferential stress at the particle surface as a function of the particle optical thickness.

$$\sigma_1 = 0.04pE\tau(\tau_* - \tau)/(1+\tau),$$
$$\tau < \tau_* = 0.6(2n-1). \tag{24}$$

To determine the particle radius a_m and optical thickness τ_m corresponding to the maximum value of σ_1, one should take into account that the power parameter p is proportional to the particle radius a. The resulting values of this optical thickness are $\tau_m \approx 1.4$ for $n = 1.5$ and $\tau_m \approx 1.7$ for $n = 2$.

6. Application to particles of selected materials

Typical examples of semi-transparent materials encountered in a wide range of high-temperature processes are ZnO and $CaCO_3$. In particular, they are used as reactants in thermochemical reactions conducted under direct high-flux solar irradiation [5,6]:

$$2\mathrm{ZnO}(s) \rightarrow 2\mathrm{Zn}(g) + \mathrm{O}_2(g) \tag{25}$$
$$\mathrm{CaCO}_3(s) \rightarrow \mathrm{CaO}(s) + \mathrm{CO}_2(g) \tag{26}$$

The importance of reaction (25) relies in the variety of applications of Zn as an energy carrier, e.g., its hydrolysis for hydrogen production. CaO is widely used in industry,

e.g., in the lime and cement production, steelmaking processing, and fine chemicals production.

As recently shown by Dombrovsky et al. [17], the following approximation based on experimental data by Yoshikawa and Adachi [18] can be used for the absorption index of ZnO:

$$k_\lambda = \begin{cases} k_0, & \lambda < \lambda_1 \\ (k_0 - k_1)/[1 + \gamma(\lambda^2 - \lambda_1^2)] + k_1, \lambda > \lambda_1 \end{cases}, \quad (27)$$

where $k_0 = 0.5$, $\lambda_1 = 0.37$ μm, and $\gamma = 120$ μm^{-2}. Two values of k_1 are selected for the parameter study: 10^{-4} (variant 1) and 5×10^{-4} (variant 2). The index of refraction is assumed constant over the entire spectrum and equal to $n = 1.9$ [18,19].

For $CaCO_3$, the absorption index is obtained by approximating experimental data by Querry et al. [20], Brewster and Kunitomo [21], and Orofino et al. [22] as

$$k_\lambda = k_0 \exp(-\gamma_1 \lambda^2) + k_1 \exp[\gamma_2(\lambda^2 - \lambda_1^2)], \quad (28)$$

where $k_0 = 0.004$, $k_1 = 0.1$, $\lambda_1 = 3$ μm, and $\gamma_1 = 10$ μm^{-2}. Two variants of the coefficient γ_2 are considered: 0.2 μm^{-2} (variant 1) and 0.15 μm^{-2} (variant 2). The index of refraction is assumed constant over the spectrum and equal to $n = 1.55$.

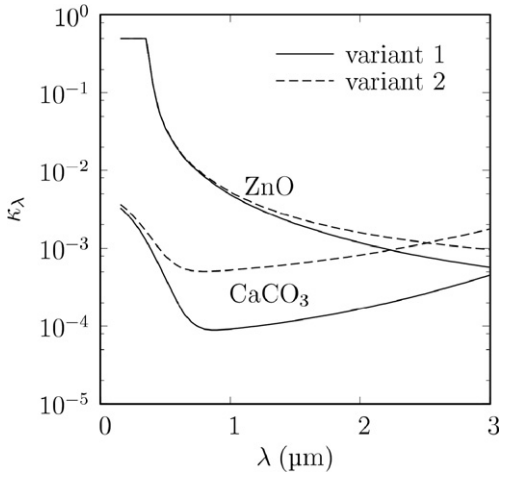

Fig. 7. Spectral index of absorption of ZnO and $CaCO_3$.

The sensitivity analysis with respect to parameters k_1 and γ_2 for ZnO and $CaCO_3$, respectively, is performed because of the considerable uncertainties in the data on the visible and near-infrared optical constants of both materials. The spectral absorption indices of ZnO and $CaCO_3$ are plotted in Fig. 7. One can see that ZnO absorbs thermal radiation much better than $CaCO_3$ in the visible and near-infrared spectral range, at least for $\lambda < 2$ μm. As a result, only very small particles of ZnO are characterized by the intensive heating of the central region, but the temperature difference and the corresponding tensile stress are small in these particles. In contrast, the low values of the absorption index of $CaCO_3$ in the visible spectral range may lead to an overheating of the central region of relatively large particles and considerable tensile stress at the particle surface.

In contrast to the qualitative analysis presented in the previous section, a full spectral solution is obtained for ZnO and $CaCO_3$ particles because of the significant spectral dependence of their optical properties. The circumferential stresses at the surface of ZnO and $CaCO_3$ particles are shown in Fig. 8 as a function of particle radius a. The following values of the physical parameters were used in the calculations: $P = 2.5$ MW/m^2, $T_s = 5780$ K (to approximate Sun's effective temperature), $T_0 = 300$ K, $\nu = 0.3$, $k_c = 3.5$ W m^{-1} K^{-1} for pure ZnO and $k_c = 1.4$ W m^{-1} K^{-1} for $CaCO_3$ [23,24]. One can see in Fig. 8a that tensile stresses in ZnO particles occur only for $a < 2.5$ μm and their values are too small for a mechanical destruction of the particle. As for particles of $CaCO_3$, the tensile circumferential stress at the particle surface is maximal for particles of radius 90–120 μm. The difference between variants 1 and 2 is substantial, demonstrating the significant dependence of the maximum tensile stress in $CaCO_3$ particles on the index of absorption.

To determine the maximum value of the tensile stress in $CaCO_3$ particles one can use the relation $\sigma_\theta = \alpha T_0 E \bar{\sigma}_1$ and

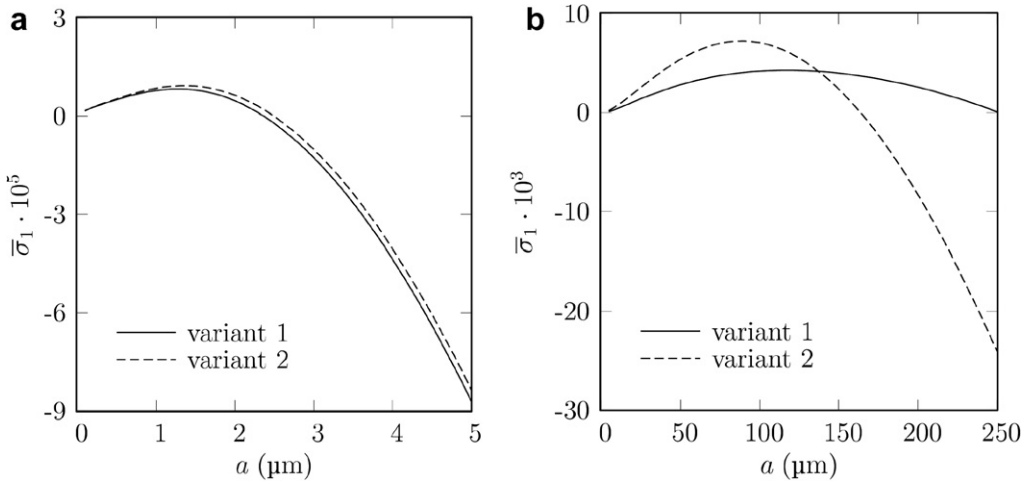

Fig. 8. The circumferential stress at the particle surface for (a) ZnO and (b) $CaCO_3$ particles as a function of the particle radius.

the calculated value of $\bar{\sigma}_1 \approx 0.007$. Substituting $\alpha = 9 \times 10^{-6}\ \mathrm{K}^{-1}$ [24] and $E = 25$ GPa [24] results in $\sigma_\theta = 0.5$ MPa. This value cannot lead to the particle destruction [25,26].

7. Conclusions

The theoretical model for the transient temperature field and thermoelastic stress–strain state of a semi-transparent spherical particle exposed to high-flux radiation has been presented. The model includes the spectral radiative transfer in a refracting and absorbing particle, the radiative–conductive heat transfer coupling and the thermoelastic stress–strain relations, but neglects the convective heat transfer. The analysis is limited to problems with spherically symmetric particle heating.

The analytical self-similar solution for temperature and thermal stress profiles in the particle is derived. This solution is applicable to the most important quasi-steady period of the particle heating. It is shown that thermal stresses during this period are independent of time. The analysis of the particle stress–strain state enables one to suggest an analytical approximation for the non-monotonic dependence of the circumferential tensile stress near the particle surface on the particle radius. The general estimate of the particle radius a_m corresponding to the maximal tensile stress is obtained.

The spectral calculations for ZnO and $CaCO_3$ particles used as reactants in high-temperature solar thermochemical processes are performed. The values of a_m are found to be very different for the two materials: about 1.5 μm for ZnO, and 100 μm for $CaCO_3$ particles. This result is explained by different absorption spectra of these substances in the visible range. It is shown that both ZnO and $CaCO_3$ particles cannot be destroyed during the rapid heating by concentrated solar radiation. However, the tensile stresses in $CaCO_3$ particles can reach considerable values. The estimates of temperature difference and thermal stresses in the particles may be interesting for more detailed analysis of the thermal decomposition of the particle material.

Acknowledgements

The first author is grateful to the Russian Foundation for Basic Research for the financial support of this work (Grants no. 04-02-16014 and 07-08-00015).

References

[1] L.A. Dombrovsky, A modified differential approximation for thermal radiation of semitransparent nonisothermal particles: application to optical diagnostics of plasma spraying, J. Quant. Spectrosc. Radiat. Transfer 73 (2–5) (2002) 433–441.
[2] L.A. Dombrovsky, M.B. Ignatiev, An estimate of the temperature of semitransparent oxide particles in thermal spraying, Heat Transfer Eng. 24 (2) (2003) 60–68.
[3] L.A. Dombrovsky, A spectral model of absorption and scattering of thermal radiation by diesel fuel droplets, High Temp. 40 (2) (2002) 242–248.
[4] A. Collin, P. Boulet, D. Lacroix, G. Jeandel, On radiative transfer in water spray curtains using the descrete ordinates method, J. Quant. Spectrosc. Radiat. Transfer 92 (1) (2005) 85–110.
[5] W. Lipiński, A. Steinfeld, Heterogeneous thermochemical decomposition under direct irradiation, Int. J. Heat Mass Transfer 47 (8–9) (2004) 1907–1916.
[6] A. Steinfeld, R. Palumbo, Solar thermochemical process technology, in: R.A. Meyers (Ed.), Encyclopedia of Physical Science and Technology, Academic Press, San Diego, 2001, pp. 237–256.
[7] L.A. Dombrovsky, W. Lipiński, Transient temperature and thermal stress profiles in semi-transparent particles heated by concentrated solar radiation, in: G. de Vahl Davis, E. Leonardi, Proceedings of the 13th Interantional Heat Transfer Conference, 13–18 August 2006, Begell House, Sydney.
[8] C.F. Bohren, D.R. Huffman, Absorption and Scattering of Light by Small Particles, Wiley, New York, 1983.
[9] P.L.C. Lage, R.H. Rangel, Total thermal radiation absorption by a single spherical droplet, J. Thermophys. Heat Transfer 7 (1) (1993) 101–109.
[10] L.A. Dombrovsky, Absorption of thermal radiation in large semi-transparent particles at arbitrary illumination of the polydisperse system, Int. J. Heat Mass Transfer 47 (25) (2004) 5511–5522.
[11] M.F. Modest, Radiative Heat Transfer, second ed., Academic Press, New York, 2003.
[12] M. Born, E. Wolf, Principles of Optics, Seventh (expanded) ed., Cambridge University Press, New York, 1999.
[13] L.A. Dombrovsky, Thermal radiation of a spherical particle of semitransparent material, High Temp. 37 (2) (1999) 260–269.
[14] L.A. Dombrovsky, Thermal radiation from nonisothermal spherical particles of a semitransparent material, Int. J. Heat Mass Transfer 43 (9) (2000) 1661–1672.
[15] L.A. Dombrovsky, Radiation Heat Transfer in Disperse Systems, Begell House, New York, 1996.
[16] B.A. Boly, J.H. Weiner, Theory of Thermal Stresses, Wiley, New York, 1960.
[17] L.A. Dombrovsky, W. Lipiński, A. Steinfeld, Approximate model for radiation heat transfer in a solar thermochemical reactor, J. Quant. Spectrosc. Radiat. Transfer 103 (3) (2007) 601–610.
[18] H. Yoshikawa, S. Adachi, Optical constants of ZnO, Jpn. J. Appl. Phys. 36 (10) (1997) 6237–6243.
[19] J. Springer, A. Poruba, M. Vanecek, S. Fay, L. Feitknecht, N. Wyrsch, J. Meier, A. Shah, T. Repmann, O. Kluth, H. Stiebig, B. Rech, Improved optical model for thin film silicon solar cells, in: B. McNelis, W. Palz, H.A. Ossenbrink, P. Helm (Eds.), Proceedings of the 17th European Photovoltaic Solar Energy Conference, Munich, 2002, pp. 2830–2835.
[20] M.R. Querry, G. Osborn, K. Lies, R. Jordon, R.M. Coveney, Complex refractive index of limestone in the visible and infrared, Appl. Opt. 17 (3) (1978) 353–356.
[21] M.Q. Brewster, T. Kunitomo, The optical constants of coal, char, and limestone, ASME J. Heat Transfer 106 (4) (1984) 678–683.
[22] V. Orofino, A. Blanco, S. Fonti, R. Proce, A. Rotundi, The infrared optical constants of limestone particles and implications for the search of carbonates on Mars, Planet. Space Sci. 46 (11–12) (1998) 1659–1669.
[23] Y.S. Touloukian, R.W. Powell, C.Y. Ho, P.G. Klemens, Thermophysical Properties of Matter, Thermal Conductivity, Nonmetallic Solids, vol. 2, IFI/Plenum, New York/Washington, 1970.
[24] Y.S. Touloukian, R.K. Kirby, R.E. Taylor, T.Y.R. Lee, Thermophysical Properties of Matter, Thermal Expansion, Nonmetallic Solids, vol. 13, IFI/Plenum, New York/Washington, 1977.
[25] A. Ersoy, U. Atici, Performance characteristics of circular diamond saws in cutting different types of rocks, Diam. Relat. Mater. 13 (1) (2004) 22–37.
[26] G.E. Exadaktylos, I. Vardalakis, S.K. Kourkoulis, Influence of nonlinearity and double elasticity on flexure of rock beams-II. Characterization of Dionysos marble, Int. J. Solids Struct. 38 (22–23) (2001) 4119–4145.